

Nonresonant charge transfer in the threshold region for ${}^3\text{He}^+ + {}^4\text{He} \rightleftharpoons {}^3\text{He} + {}^4\text{He}^+$

M. M. Schauer,* S. R. Jefferts,* and G. H. Dunn†

*Joint Institute for Laboratory Astrophysics, University of Colorado and National Institute of Standards and Technology,
Boulder, Colorado 80309-0440*

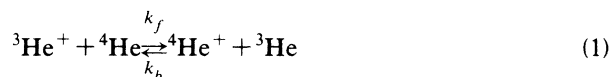
(Received 7 June 1990)

Measurements of the ratio of the rate coefficient for charge transfer between ${}^3\text{He}^+$ and ${}^4\text{He}$ to that for the reverse process have been made in the temperature range $8\text{ K} \lesssim T \lesssim 80\text{ K}$. A 1.1-meV difference in the ionization potential of these species leads to an endothermicity in the forward direction of this reaction, and these experiments constitute the only measurements of a threshold resulting from such a small endothermicity. In addition, a limited number of direct measurements of the rate coefficients for these processes have been made and are included here. The measurements were done in a cooled Penning trap using Fourier transform spectroscopy of the axial trapping frequency. The measurements are compared to theoretical estimates.

INTRODUCTION

Low-energy studies of charge transfer between helium ions and atoms have been restricted to energies above 100 meV.¹⁻³ In this region, the cross section is found to increase with decreasing collision energy, in agreement with theoretical predictions.^{4,5}

Very little work has been done on charge exchange involving ${}^3\text{He}$ and ${}^4\text{He}$ ions and atoms. Due to the difference in reduced mass, the ionization potential of ${}^3\text{He}$ is less than that of ${}^4\text{He}$ by approximately 1.1 meV. Hence the processes



are nonresonant charge-transfer processes. Since the forward reaction is endothermic, one would expect the cross section for this process to exhibit a threshold at 1.1 meV. Since in our apparatus the energy distribution is essentially⁶ Maxwell-Boltzmann, the ratio of the rate coefficient for the forward reaction to the rate coefficient for the backward reaction should approach zero at temperatures below 13 K and rise to unity with increasing temperature.

Rundel *et al.*³ have made merged-beams cross-section measurements for the process ${}^3\text{He}^+ + {}^4\text{He} \rightarrow {}^3\text{He} + {}^4\text{He}^+$ for energies from 0.1 to 187 eV and, as expected, find no difference between the cross sections for this process and the resonant process, ${}^4\text{He}^+ + {}^4\text{He} \rightarrow {}^4\text{He} + {}^4\text{He}^+$, so called because there is zero energy difference between the two sides of the reaction. More recently, Kartoshkin⁷ has performed thermal measurements at 77 K of the rate coefficient for ${}^3\text{He} + {}^4\text{He}^+ \rightarrow {}^3\text{He}^+ + {}^4\text{He}$ and for the resonant process involving ${}^3\text{He}$. His measurements show the rate coefficient for the nonresonant process to be 0.87 that for the resonant process.

We have conducted experiments on this system at temperatures $8\text{ K} \lesssim T \lesssim 80\text{ K}$, thus covering the threshold re-

gion. These experiments are characterized by well-defined temperatures and they were conducted at neutral reactant gas pressures at which three-body effects are negligible.

EXPERIMENTAL TECHNIQUE

The measurements described here were done using a Penning ion trap described in detail elsewhere.⁶ However, due to the rapidity of these reactions and the expected strong temperature dependence of the rate coefficient of the forward reaction, the bolometric detection scheme⁶ used in previous experiments in this trap could not be used. We give a brief description of the trap before discussing the detection scheme used.

The ion trap sits in the bore of a superconducting solenoid and is thermally anchored to the walls of the liquid-helium Dewar through a thermal impedance. A resistive wire wound directly onto the trap electrodes allows the temperature of the ion cloud environment to be set at temperatures $8\text{ K} \lesssim T \lesssim 80\text{ K}$. Reactant gases are introduced through a pipe that is thermally anchored to the trap electrodes thus ensuring that the neutral gas in the trap volume is in thermal equilibrium with the trap. Adjacent to the trap is a cryopump for excess gases.

The motion of ions in a Penning trap has been discussed in great detail in the literature;⁸⁻¹⁰ it suffices here to say that the motion of an ion along the trap axis is harmonic with frequency proportional to $(V_a q/m)^{1/2}$, where V_a is the applied trapping voltage, and q/m is the charge to mass ratio of the ion. This harmonic motion of the ions induces image currents in the endcaps.

Normally the ion motions are randomly distributed in phase, and the image currents are incoherent. However, if the ions are driven resonantly at the axial frequency ω_z they can be made to oscillate in phase with each other. The resulting signal on the endcap for N ions of the same charge to mass ratio is

$$S = [C\alpha(\omega_z)qN\tau/m]\cos(\omega_z t), \quad (2)$$

where C is a constant depending on the trap geometry and the amplitude of the drive signal, α is the frequency-dependent detector gain, q/m the charge to mass ratio of the ions, and τ the length of time the ions are resonantly driven. This assumes that the ion kinetic energy remains small compared to the trap well depth throughout the detection process as is the case in these experiments. Resonantly driven motion of the ions along the z axis together with Fourier transform analysis has also been recently described by Schweikhard *et al.*¹¹

For an ion cloud consisting of several ion species of different charge to mass ratio, the ions of each species can be made to oscillate in phase with each other, but independently from the ions of the other species, by resonantly driving each species at its characteristic axial frequency. This necessitates sweeping the frequency of the resonant drive signal. Great care must be taken to assure that all the ion species are in resonance with the drive signal for the same length of time, and the manner in which this was accomplished is described in detail else-

where.¹²

If the cloud consists of two singly charged ion species of different masses, as in these experiments, then the total signal is

$$S = C\{[\alpha(\omega_{z_1})N_1\tau/m_1]\cos(\omega_{z_1}t) + [\alpha(\omega_{z_2})N_2\tau/m_2]\cos(\omega_{z_2}t)\}, \quad (3)$$

where N_1 and N_2 are the numbers of ions of species 1 and 2, respectively, m_1 and m_2 their masses, ω_{z_1} and ω_{z_2} are their unshifted axial oscillation frequencies, and there is an arbitrary phase between the oscillation of the two species which is taken as zero at $t=0$ in this equation. This phase is of no relevance here, as we measure the power at the frequencies ω_{z_1} and ω_{z_2} over many cycles of each frequency.

We define the frequencies $\omega_A = (\omega_{z_1} + \omega_{z_2})/2$, the average axial frequency, and $\omega_D = (\omega_{z_2} - \omega_{z_1})/2$, one-half the separation of the two frequencies. Then Eq. (3) can be written as

$$S = C\tau\{[\alpha(\omega_{z_1})N_1/m_1][\cos(\omega_D t)\cos(\omega_A t) - \sin(\omega_A t)\sin(\omega_D t)] + [\alpha(\omega_{z_2})N_2/m_2][\cos(\omega_A t)\cos(\omega_D t) + \sin(\omega_A t)\sin(\omega_D t)]\}. \quad (4)$$

Hence the signal consists of a rapid oscillation at the average axial frequency of the two ions with a slow modulation at one-half the difference frequency. From the Fourier transform of this signal one is able to find the relative number of ions of each species provided the detector transfer function is known. Figure 1 shows such an ion signal from our trap along with its Fourier transform. This method will be referred to as the beat signal method throughout the remainder of the paper.

It is also possible to cause the center of mass of the cloud to oscillate at the axial frequency of an ion of mass $N\bar{m}$ and charge Nq ,

$$v = K(qV/\bar{m})^{1/2}, \quad (5)$$

where K is a constant, V is the trapping voltage, N is the total number of ions, and \bar{m} is the average mass of the ions. For a cloud of two components of masses m_1 and m_2 with species one having fractional abundance of ϕ , the average mass is

$$\bar{m} = \phi m_1 + (1 - \phi)m_2. \quad (6)$$

Using this relation it is possible to determine the relative abundances of the ion species from the average-mass frequency. Experiments done on clouds of known composition of ${}^3\text{He}^+$ and ${}^4\text{He}^+$ confirm Eq. (5). This method will be referred to as the average-mass method in the remainder of the paper.

In the work reported here, two different types of measurements were made. Direct measurements of the rate coefficients for both reactions were made over the temperature range of 15–50 K. In addition, measurements

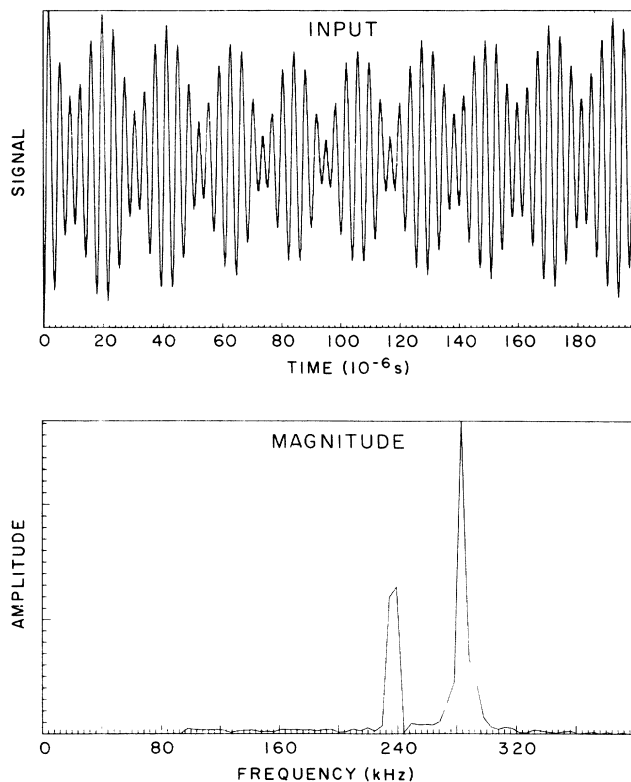


FIG. 1. Ion beat signal and its Fourier transform for a cloud of ${}^3\text{He}^+$ and ${}^4\text{He}^+$ ions.

of the ratio of the rate coefficient for the forward reaction to that for the backward reaction were made over the temperature range 8–80 K.

Direct measurements

The direct measurements were made using the average-mass method. In these measurements, an initial sample of ${}^3\text{He}^+$ or ${}^4\text{He}^+$ ions was made by electron bombardment, and neutral ${}^4\text{He}$ or ${}^3\text{He}$ gas was introduced, respectively. The axial oscillation frequency was then monitored as it evolved from the frequency of a pure cloud of parent ions to that of a pure cloud of product ions. From this time evolution of the axial oscillation frequency the time evolution of the cloud contents was then derived as explained in the discussion of the average-mass method, and the rate coefficient was extracted from this information.

It is important to note that the detection process results in an insignificant heating to the ion cloud. Any heating of the cloud above the ambient temperature during the reaction results in an effective reaction temperature higher than the ambient temperature. Obviously, this leads to an incorrect assignment of temperature to the measured rate coefficient. The extent to which the effective reaction temperature deviates from the ambient temperature is a function of the maximum temperature achieved by the cloud during ion detection and the fraction of the total reaction time spent at the elevated temperature.

Tests indicated that the temperature of the cloud increased less than 5 K during detection. The cloud then cooled to the ambient temperature in 5 to 10 s through ion–neutral-atom collisions. Since the reaction typically required about 600 s to reach completion, during which time the cloud was interrogated five or six times, the fraction of time the cloud spent at the slightly elevated temperature was small. Hence both the extent and duration of temperature elevation were minimal, and the deviation of the effective reaction temperature from the ambient temperature resulted in only a small correction to the reaction temperature.

Due to the high rate coefficient, very low neutral densities were necessary ($\approx 10^7 \text{ cm}^{-3}$). However, due to the limited helium pumping capacity of the cryopump, the background density slowly increased over several days of experiments, increasing from $\lesssim 10^4 \text{ cm}^{-3}$ to roughly 10^7 cm^{-3} . As the ${}^3\text{He}$ -to- ${}^4\text{He}$ ratio in this background gas was unknown, the *direct rate measurements* could only be done early in an experiment before the background density became too high.

Ratio measurements

For a mixture of neutral ${}^3\text{He}$ and ${}^4\text{He}$, an equilibrium will be established between the forward and backward reactions allowing the *ratio of the forward to backward rate coefficients* to be measured. For a given mixture of neutral ${}^3\text{He}$ and ${}^4\text{He}$ gas, the ratio of rate coefficients is given by

$$\frac{k_f}{k_b} = \frac{[{}^3\text{He}]N({}^4\text{He}^+)}{[{}^4\text{He}]N({}^3\text{He}^+)}, \quad (7)$$

where the brackets refer to the density of neutral gas in the trapping region, and the number of ions of mass m is indicated by $N({}^m\text{He}^+)$.

The effects of the background of unknown ${}^3\text{He}$ -to- ${}^4\text{He}$ ratio can be minimized in these measurements, since high neutral gas densities can be used. Thus densities at least ten times the background density were used in these ratio measurements. Hence, in the worst case, the background gas accounted for 10% of all ion–neutral-atom collisions.

In these experiments a known mixture of ${}^3\text{He}$ and ${}^4\text{He}$ was made in the gas handling system. Reactant ions were made in the trap by electron bombardment of neutral gas. The gas mixture was then introduced, thus cooling the cloud to the reaction temperature and establishing the equilibrium mixture of He ions. The majority of the ratio measurements were done using the beat signal method, although some were done using the average-mass method. Each measurement was repeated several times before a new mixture of neutral gas was used. Hence the data points for k_f/k_b at each temperature are the results of several measurements with neutral ${}^3\text{He}$ -to- ${}^4\text{He}$ ratios varying over as much as a factor of 10.

In these ratio measurements heating of the cloud caused no problem, since the time scale for driving and detecting the ions was at least 1000 times shorter than either the reaction time constant or the collision time constant. Hence the measured rate coefficient ratio is the ratio for the ambient temperature and not that for some elevated temperature reached as a result of the detection process.

RESULTS AND DISCUSSION

In general, the cross section for resonant charge transfer decreases with increasing collision speed due to the decreased collision duration at higher velocities. The nonresonant charge-transfer cross section, on the other hand, increases with increasing collision speed eventually reaching a maximum and merging with the corresponding resonant curve. This behavior is well understood, and the position of the maximum of the cross section can be estimated by the well-known Massey adiabatic criterion.^{13,14} In addition, some theoretical models^{4,15} have been developed that model this behavior with some success, though not distinguishing between the exoergic and endoergic processes. However, for collision energies less than the resonance defect, the endothermic reaction cannot occur, and the cross section for this process will fall to zero more rapidly than the predictions of these theories. The exothermic process should still be adequately described by these theories.

We can calculate the above-threshold nonresonant charge-transfer cross section for reactions (1) using the result by Demkov.¹⁵ Demkov calculated the charge-transfer probability $P_0(v)$ as a function of collision velocity for zero-impact-parameter collisions. The cross section can be derived from the charge-transfer probability by integrating the probability over all possible impact pa-

rameters.

Charge transfer can only occur while the wave functions of the colliders overlap, and all collisions with impact parameters less than some critical value b_c will lead to such overlap. Work on other systems¹⁶ indicates that the charge-transfer probability is roughly constant as a function of impact parameter out to this critical value. We therefore take the probability of charge transfer for all collisions with impact parameter less than b_c to be the zero impact parameter value from Demkov's result. The cross section for this process then is $\sigma(v) = \pi b_c^2 P_0(v)$.

At high energies, ion-induced dipole effects and the He-He⁺ interaction potential do not cause significant deviation of the collision trajectories from straight lines, and one can use the diameter of the helium atom for b_c . In the low-energy collisions reported here, significant bending of trajectories occurs, and this value of b_c leads to a vast underestimate of the cross section. A more representative value for b_c can be obtained by averaging the cutoff impact parameter for orbiting collisions, $b_0 = (q^2\alpha / 2\pi\epsilon_0 E_T)^{1/4}$, over the range of collision energies under study here. Impact parameters less than b_0 lead to collisions in which the projectile spirals inward and "bounces off" the hard repulsive core of the target, thus allowing for charge transfer. In this expression, q is the ionic charge, α is the neutral polarizability, ϵ_0 is the permittivity of free space, and E_T is the translational kinetic energy.

Since Demkov's calculations were for above-threshold energy collisions, we take the cross section calculated as described above to be that for the exothermic process, i.e., the backward reaction in reactions (1). An expression for the endothermic cross section in terms of the exothermic one can be obtained by use of detailed balance. The resulting cross sections are shown in Fig. 2. The resonant curve indicated in this figure is an extrapolation of the form $\sigma = (5.09 - 0.299 \ln E_T)^2$ which is the best-fit re-

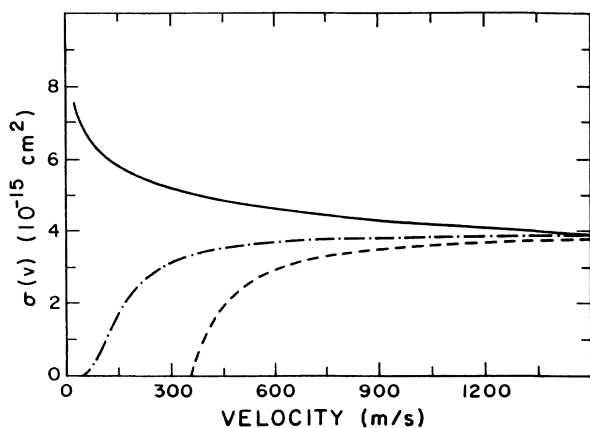


FIG. 2. Theoretical prediction of cross section for charge transfer as a function of velocity in the ³He-⁴He system. This is based on the theory of Demkov. The dashed-dotted line is the curve for exothermic reaction and the dashed line for the endothermic reaction. The solid line is an extrapolation of the data of Rundel *et al.* (Ref. 3) for resonant charge transfer.

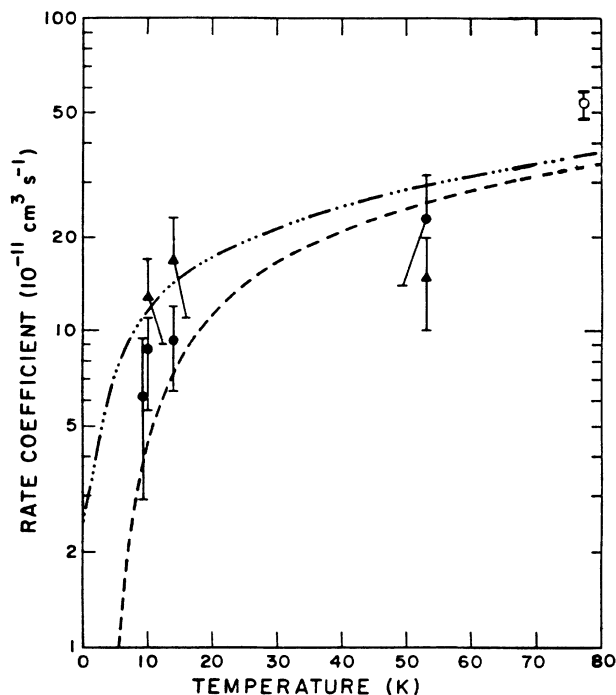


FIG. 3. Measured values of exothermic rate coefficient (triangles) and endothermic rate coefficient (dots). The open circle is the result of Kartoshkin (Ref. 7). Theoretical estimates are given by dashed line (endothermic reaction) and dashed-dotted line (exothermic reaction).

sult that Rundel *et al.*³ find for their data. We use these cross-section curves in the expression for the rate coefficients, $k = \int v\sigma(v)f(v)dv$, where $f(v)$ is the Maxwell-Boltzmann velocity distribution.

Figures 3 and 4 show the results for the measurements and calculations of the rate coefficients and their ratios, respectively. The agreement of the measured and calculated rate coefficients is reasonable, although the theory seems to underestimate the rate coefficient at low temperatures and overestimate it for the highest-temperature measurements. This is not surprising in view of the average value of b_0 used in the derivation of the cross section. One may expect that because interaction potential effects on orbits will be greater as the velocity decreases, the choice of an average b would lead to an underestimate at low temperatures and an overestimate at high. In the case of the ratio measurements, one expects better agreement, as the critical impact parameter b_c cancels out. This is indeed the case, as can be seen from Fig. 4, which shows excellent agreement between the measured and calculated ratios except for the very lowest-temperature point.

The rate coefficient ratio is, of course, just the equilibrium constant for the reactions (1) and must equal $\exp(-\Delta/kT)$, where Δ is the resonance defect. A plot of the natural logarithm of the rate coefficient ratio as a function of $1/T$, a van't Hoff plot, is shown in Fig. 5. Again, the agreement between the data and the expected

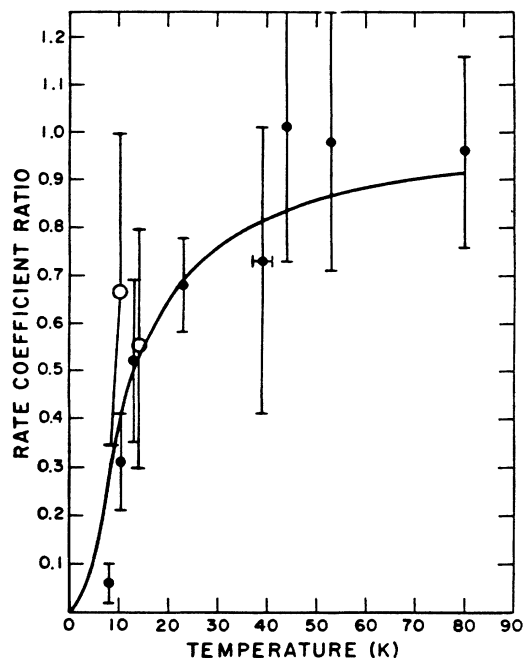


FIG. 4. Measured ratio of the rate coefficient for endothermic reaction to that for exothermic reaction (dots). Open circles are ratios calculated from measured rate coefficients. Solid line is calculated value based on theory of Demkov.

straight-line behavior is excellent except for the lowest-temperature point. A least-squares fit to the data yields $\Delta = 1.4 \pm 0.3$ meV, consistent with the expected value. The resulting line is shown as the dashed line in Fig. 5.

As can be seen from both Figs. 4 and 5, the lowest-temperature point exhibits the worst agreement with theoretical predictions. Obviously, the equilibrium is displaced in the direction of ${}^3\text{He}^+$ more at this temperature than at the higher temperatures reported here. As a result, the two peaks in the Fast Fourier transform are the hardest to separate at this temperature, and the ratio measurements are more difficult to make. This difficulty is reflected in the nearly 70% error bars of this lowest-temperature point in Fig. 3. Omission of this point from the least-squares fit of Fig. 5 yields $\Delta = 1.1 \pm 0.3$ meV, which is in excellent agreement with the expected value. This is shown by the solid line.

The otherwise good agreement between theory and ex-

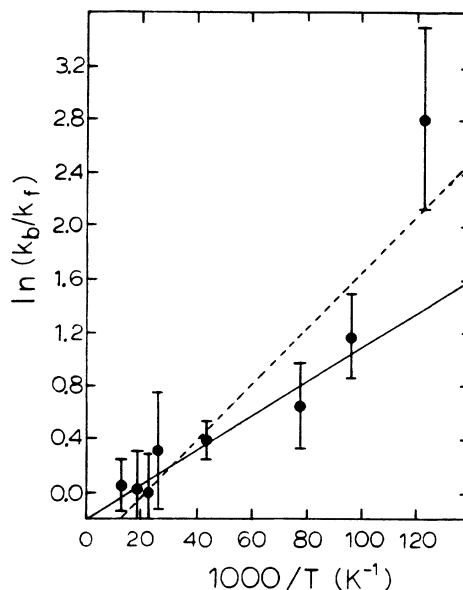


FIG. 5. van't Hoff plot for the ratio data. The dashed line is a best fit to all the data, while the solid line omits the lowest-temperature point.

periment found here confirms the picture of this reaction as a nonresonant charge-transfer process with resonance defect of 1.1 meV. Furthermore, the excellent agreement of the ratio data with the ratios calculated on the basis of Demkov's theory and detailed balance suggests that Demkov's theory may be applied to low-energy collisions below threshold for the exothermic channel of charge-transfer reactions such as reactions (1). At the same time, the discrepancy between the measured and calculated rate coefficients shows that interaction potential effects will always be a serious difficulty for this approach and that full trajectory modeling is necessary for a complete understanding of this system.

ACKNOWLEDGMENTS

The authors acknowledge John Briggs for helpful conversations. The research was supported in part by National Science Foundation Grant No. PHY86-04504 to the University of Colorado.

*Also with Department of Physics, University of Colorado, Boulder, CO 80309-0440.

†Quantum Physics Division, National Institute of Standards and Technology.

¹P. Mahadevan and G. D. Magnuson, Phys. Rev. **171**, 103 (1968).

²H. Helm, J. Phys. B **10**, 3683 (1977).

³D. R. Rundel, D. E. Nitz, K. A. Smith, R. W. Geis, and R. F. Stebbings, Phys. Rev. A **19**, 33 (1979).

⁴D. Rapp and W. E. Francis, J. Chem. Phys. **37**, 2631 (1962).

⁵D. P. Hodgkinson and J. S. Briggs, J. Phys. B **9**, 255 (1976).

⁶S. E. Barlow, J. A. Luine, and G. H. Dunn, Int. J. Mass Spectrom. Ion Proc. **74**, 97 (1986).

⁷V. A. Kartoshkin, Pis'ma Zh. Eksp. Teor. Fiz. **45**, 126 (1987) [JETP Lett. **45**, 154 (1987)].

⁸J. Byrne and P. S. Farago, Proc. Phys. Soc. London **86**, 801 (1965).

⁹L. S. Brown and G. Gabrielse, Rev. Mod. Phys. **58**, 233 (1986).

¹⁰F. L. Walls and G. H. Dunn, Physics Today **27**(8), 30 (1974).

¹¹L. Schweikhard, M. Blundschling, R. Jertz, and H.-J. Kluge, Int. J. Mass Spectrom. Ion Proc. **89**, R7 (1989).

¹²M. Schauer, Ph.D. thesis, University of Colorado, Boulder,

- 1990.
- ¹³H. S. W. Massey and E. H. S. Burhop, *Electronic and Ionic Impact Phenomena* (Clarendon, Oxford, 1956).
- ¹⁴J. B. Hasted, *Physics of Atomic Collisions* (Butterworth, Washington, D.C., 1964).
- ¹⁵Yu. N. Demkov, *Zh. Eksp. Teor. Fiz.* **45**, 195 (1963) [Sov. Phys.-JETP **18**, 138 (1964)].
- ¹⁶J. S. Briggs, *Rep. Prog. Phys.* **39**, 217 (1976).